

Signatures of integrability in charge and thermal transport in 1D quantum systems

Subroto Mukerjee^{1,2} and B. Sriram Shastry³

¹*Department of Physics, University of California, Berkeley, CA 94720*

²*Materials Sciences Division, Lawrence Berkeley National Laboratory, Berkeley, CA 94720*

³*Department of Physics, University of California, Santa Cruz, CA 95064*

Integrable and non-integrable systems have very different transport properties. In this work, we highlight these differences for specific one dimensional models of interacting lattice fermions using numerical exact diagonalization. We calculate the finite temperature adiabatic stiffness (or Drude weight) and isothermal stiffness (or “Meissner” stiffness) in electrical and thermal transport and also compute the complete momentum and frequency dependent dynamical conductivities $\sigma(q, \omega)$ and $\kappa(q, \omega)$. The Meissner stiffness goes to zero rapidly with system size for both integrable and non-integrable systems. The Drude weight shows signs of diffusion in the non-integrable system and ballistic behavior in the integrable system. The dynamical conductivities are also consistent with ballistic and diffusive behavior in the integrable and non-integrable systems respectively.

PACS numbers: 72.10 -d, 72.10 Bg

A perfect metal is distinguished from a superconductor by the absence of the Meissner effect, although both share an infinite conductivity at zero frequency. In one dimension, another fundamental kind of metallic systems is possible, corresponding to an integrable system. We term this as an integrable metal (IM) and such a system can display characteristics that are different from both a perfect metal and a superconductor, such as an infinite conductivity *at all temperatures*. In contrast, a perfect but non integrable metal (NIM) becomes resistive at finite temperatures due to inelastic collisions and umklapp. We track this difference between an IM and NIM directly in this work by calculating various transport stiffnesses also the dynamical conductivities for both charge and energy using numerical exact diagonalization and a suitably generalized Kubo formula [1]. The main result is that the NIM shows evidence of diffusive behavior in both the static and dynamic conductivities, while the IM shows several signs of ballistic transport.

The adiabatic stiffness (or Drude weight) is given by [1]

$$\bar{D}_\alpha = \frac{1}{L} \left[\langle \Gamma_\alpha \rangle - \hbar \sum_{n,m} (1 - \delta_{\epsilon_n, \epsilon_m}) \frac{p_n - p_m}{\epsilon_m - \epsilon_n} |\langle n | J_\alpha | m \rangle|^2 \right], \quad (1)$$

Here $\Gamma_\alpha = -\lim_{k \rightarrow 0} \frac{1}{k} [J_\alpha(k), K_\alpha(-k)]$, where $K_\alpha(k)$ is the Fourier component of a local density operator ($\alpha = e$ for the charge density, $\alpha = E$ for the energy density and $\alpha = Q$ for the heat density) while $J_\alpha(k)$ is that of the corresponding current operator. Here $p_n = e^{-\beta \epsilon_n} / Z$ is the Boltzmann weight of the many-body state with energy ϵ_n and Z , the partition function. This arises in the adiabatic evolution of an equilibrium state disturbed in the infinitely remote past by the application of a time-dependent perturbation, and is the coefficient of the delta function in the conductivity for charge transport.

Another stiffness, the isothermal (or “Meissner”) stiffness D_α can be defined by the same expression as Eqn. 1 by omitting the Kronecker delta function that forbids

equal energy states. For charge transport, this arises in a study of the Byers-Yang type curvature of the free energy with respect to a flux through the ring [2]. On general grounds, a superconductor which displays the Meissner effect has a non-zero value of D_e . While a non-vanishing D_α implies a non-vanishing \bar{D}_α , the converse is not true.

The distinction between D_α and \bar{D}_α resides in the relative statistical weight of states with equal energy. It also follows that if D_α is known to vanish, then \bar{D}_α can be written as a sum over only equal energy states

$$\begin{aligned} \bar{D}_\alpha &= \frac{\hbar}{k_B T L} \sum_{\epsilon_n = \epsilon_m} p_n |\langle n | J_\alpha | m \rangle|^2 \\ &= \bar{D}_\alpha^d + \bar{D}_\alpha^{nd} \end{aligned} \quad (2)$$

The current operator commutes with the crystal momentum, so n and m have the same value of crystal momentum q . In general, an IM, can have degeneracies among states with same q due to the presence of dynamical symmetries. We can thus write \bar{D} as the sum of \bar{D}_α^d , the contribution from states degenerate with others *at the same value of q* and \bar{D}_α^{nd} , the contribution from states with no degeneracies *within the same* crystal momentum sector.

In an interesting paper [3], it has been argued that in an IM with time reversal invariance, a non-zero value of \bar{D}_e is due to the presence of a large number of current carrying states, which are degenerate with a partner state at the opposite value of q . An important question is how these current carrying states contribute to \bar{D}_α^d and \bar{D}_α^{nd} : What is the role of the dynamical symmetries in determining the magnitude of the adiabatic stiffness? This is especially relevant when time reversal is broken by e.g. an irrational flux through the ring, as used here, whereby even non-degenerate states *can carry currents*.

We have been motivated by these questions to undertake an exhaustive numerical study of a typical IM and NIM, by computing their exact energy spectra and all the current matrix elements and consequently the transport

stiffnesses and dynamic conductivities. This exercise is done in 1D with a popular model, the $t - t' - V$ model of spinless fermions, where a single non-zero parameter t' destroys the integrability, but lets the system remain a perfect metal (an NIM). All stiffnesses are generally non-zero for finite systems, and it is only the systematics of their size dependence that gives us reliable information on the large size behavior. We also study for the first time, the complete dynamic conductivity $\sigma(q, \omega)$ and thermal conductivity $\kappa(q, \omega)$ in an IM and NIM, using an appropriate scheme for binning the discrete data points to obtain continuous functions.

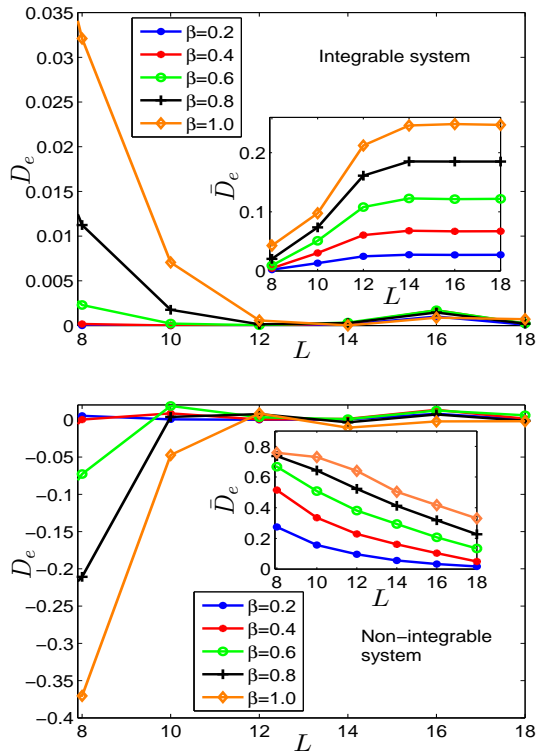


FIG. 1: (Top) The isothermal and adiabatic (inset) stiffness for electrical transport in the integrable system at various values of β with an irrational flux twist. It can be seen that the former tends to zero rapidly with increasing system size while the latter appears to go to a constant, indicative of ballistic transport. (Bottom) The same stiffnesses for electrical transport in the non-integrable system again with an irrational flux twist. Both tend to zero with system size but D_e does so more rapidly.

The $t - t' - V$ model of spinless fermions on a 1D ring is given by the Hamiltonian

$$H = -t \sum_j (c_{j+1}^\dagger c_j + c_j^\dagger c_{j+1}) - t' \sum_j (c_{j+2}^\dagger c_j + c_j^\dagger c_{j+2}) + V \sum_j (n_j - 1/2)(n_{j+1} - 1/2). \quad (3)$$

For concreteness, we choose the value of t and V to

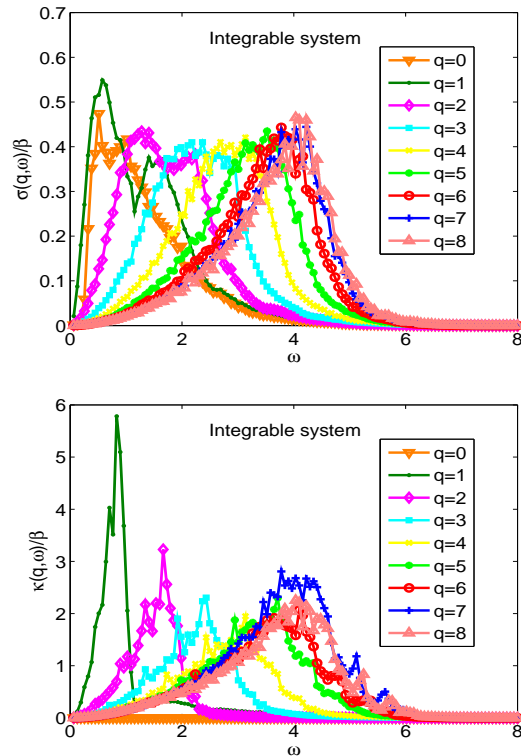


FIG. 2: Plots of $\sigma(q, \omega)$ (above) and $\kappa(q, \omega)$ (below) vs. ω for the integrable system with $L = 16$ at $\beta = 0.001$. It can be seen in the plot of $\kappa(q, \omega)$ that there is a band of frequencies for a given value of q in which the value of $\kappa(q, \omega)$ is large and then abruptly falls to zero at the boundaries. This behavior is much less pronounced in $\sigma(q, \omega)$.

be 1.0 and 2.0 respectively. With $t' = 0$, this model can be mapped onto the integrable spin 1/2 Heisenberg ring using the Jordan-Wigner transformation. We set $t' = 1$ when we model the NIM. Chains of length 6-18 are studied and we focus on half-filling for definiteness. The Hamiltonian Eqn. 3 is then numerically diagonalized exactly. We would like to emphasize that our conclusions vis a vis integrability and non-integrability are quite general and independent of the microscopic parameters and the filling. We also apply an irrational flux twist to break time-reversal invariance, which too does not affect the integrability. *For convenience, we will henceforth use the term non-degenerate only for states which are not degenerate with any other state at the same q .* With the irrational flux twist, the NIM now has only non-degenerate states while the IM has both degenerate and non-degenerate states. This has the advantage of enabling us to analyze the behavior of the IM in contrast to the NIM, mainly in terms of degeneracies (and set $\bar{D}_e^d = 0$ for the NIM). We calculate D_α and \bar{D}_α for electrical and thermal transport at different temperatures ($T = 1/\beta$ is measured in units of t).

We show here only the results for electrical transport

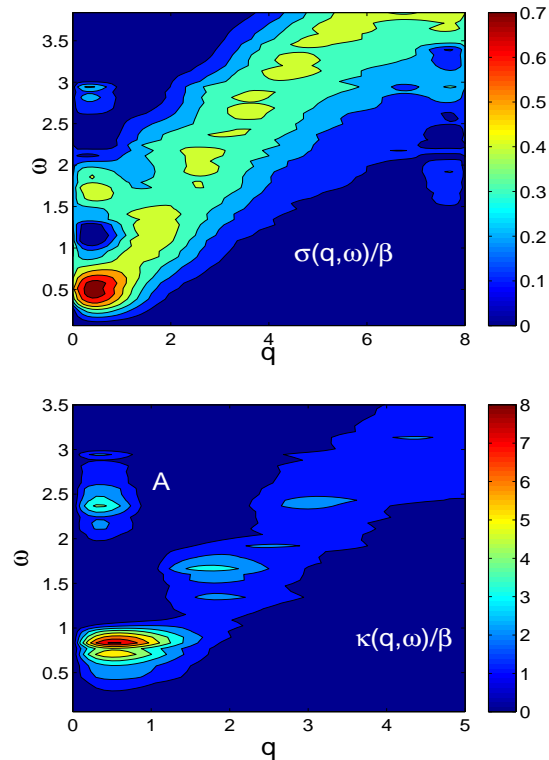


FIG. 3: Colored contour plots of $\sigma(q, \omega)$ (above) and $\kappa(q, \omega)$ (below) for the IM with $L = 16$ at $\beta = 0.001$. Momentum ($q = 0$ to 8). An eighth order polynomial interpolation has been used to convert the discrete numerical data into a function of a continuous momentum variable q and the feature marked A on the lower plot is an artifact of that. The plot of $\kappa(q, \omega)$ shows the banded continuum in the center bounded by dark blue regions.

in Fig. 1, but the ones for thermal transport display exactly the same qualitative behavior. The issue of whether the charge stiffness (\bar{D}_e in our model) in the Heisenberg ring ($t' = 0$) is actually non-zero at finite temperature remains contentious [4, 5]. Our results up to the largest system size ($L = 18$) seem to indicate that it is non-zero. Indeed, the overall picture that emerges is consistent with ballistic transport. A confirmation of this to rule out any slow (logarithmic) decay with L is currently beyond the range of accessible system sizes. The NIM on the other hand shows a clear (exponential at high temperature) decay of \bar{D}_e with system size indicating diffusion. This behavior persists to temperatures higher than the typical energy scales in the problem and *in fact even up to infinite temperature*. These results are interesting since they show that the system is aware of its integrability or non-integrability even up to infinite temperature. D_e vanishes rapidly in the thermodynamic limit in both systems (even without the flux twist). This shows in particular that the IM despite having an infinite conductivity at $\omega = 0$ is not a superconductor. It is a curious fact

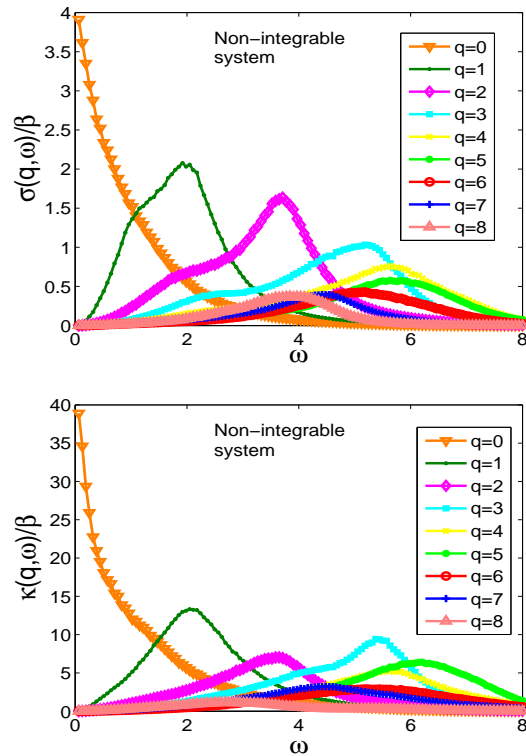


FIG. 4: Plots of $\sigma(q, \omega)$ (above) and $\kappa(q, \omega)$ (below) vs. ω for the NIM with $L = 16$ at $\beta = 0.001$. $\kappa(q, \omega)$ no longer displays the banded behavior of the integrable system and falls off gradually (and not abruptly) at higher frequencies. The peaks in both $\sigma(q, \omega)$ and $\kappa(q, \omega)$ at large q are also present in the density-density correlation functions indicating the presence of overdamped excitations.

that D_e is positive at small system sizes in the IM and negative in the NIM. The situation is reversed without a flux twist. The transport stiffnesses in small systems can in general have either signs depending on the microscopics [6].

We now outline a statistical study of \bar{D}_e in the two systems. Since the Meissner stiffness D_e is zero at large L , \bar{D}_e is given by Eqn. 2. To enable a comparison of \bar{D}_e in the IM and the NIM at a given L , we remove the dependence on microscopic parameters (i.e. normalize) by dividing by Γ_e . We also normalize \bar{D}_e^d and \bar{D}_e^{nd} in the same way. For the largest system sizes ($L = 18$), we find that the normalized \bar{D}_e is about 8-15 times larger in the IM than the NIM for the values of β considered. One can now ask the question we set out to answer in a slightly different form: Are the large current carrying states which give a large (normalized) \bar{D}_e in the IM compared to the NIM in the degenerate states in the former, or in the non-degenerate ones? This can be answered by comparing the magnitudes of the normalized \bar{D}_e^d and \bar{D}_e^{nd} .

Motivated by this question, we have studied the statis-

tics of the number of degeneracies and the the current matrix elements in the two systems. We find that at $L = 18$ in the IM, about 10% of the states are pairwise degenerate with a very negligible fraction of higher order degeneracies. Further, most of the degeneracies occur among states with total lattice momentum 0 or π . The ratio of the normalized $\bar{D}_e^d/\bar{D}_e^{nd}$ is at most 0.2 for the values of β investigated. On the other hand, the ratio of \bar{D}_e^{nd} between the IM and the NIM is about 8-15. Thus, we come to the following interesting conclusion: Even though the IM has degeneracies, their contribution to the charge stiffness is not significant. *The large current carrying states are primarily among the non-degenerate states.* We also note that the eigenvalues of the current operator in a given degenerate sector in the IM, are always roughly of the same magnitude. We reiterate that the term non-degenerate is used here only for states with no degeneracies *within* a sector of total momentum q . Thus, it appears the presence of dynamical symmetries does not have a direct effect on the charge stiffness through the creation of degenerate states. A more detailed account of the statistics alluded to above will be presented elsewhere.

We now focus on transport at finite frequency (ω) and q . The q and ω dependent conductivities are given by

$$A_\alpha(q, \omega) = c(\omega) \sum_{p, \epsilon_n \neq \epsilon_m} p_n |\langle n | J_\alpha(q) | m \rangle|^2 \delta(\epsilon_m - \epsilon_n - \hbar\omega), \quad (4)$$

where $c(\omega) = \frac{\pi}{L} \left(\frac{1 - e^{-\beta\omega}}{\omega} \right)$, $A_e(q, \omega) = \sigma(q, \omega)$ and $A_E(q, \omega) = \kappa(q, \omega)$. These conductivities can also be related to density-density correlation functions of the charge and energy [5]. We choose a small value of $\beta = 0.001$ since for a calculation of this sort, numerical exact diagonalization is most efficient only at very high temperatures [7]. The irrational flux twist turns out to be unimportant to the results here. $\sigma(q, \omega)$ and $\kappa(q, \omega)$ as functions of ω (in units of the hopping t) for different values of q (going from 0 to 8) for an $L = 16$ IM are shown in Fig. 2. $\kappa(q = 0, \omega) \propto \delta(\omega)$ since $[J_E(q = 0), H] = 0$ but $[J_e(q = 0), H] \neq 0$ and thus $\sigma(q = 0, \omega)$ has some structure at $\omega \neq 0$. A more interesting feature is that $\kappa(q, \omega)$ is non-zero only within a band of frequencies for small values of q and goes to zero abruptly at the boundaries of the band. Moreover, this band shifts to higher frequencies with increasing q . The dispersion of these banded modes appears to be roughly linear (at small q), consistent with considerations of ballistic transport. The situation is similar to the case of free fermions where ballistic transport causes a similar banded structure in $\kappa(q, \omega)$. The common feature of this IM and free fermions is integrability, which it appears is strongly associated with the concept of ballistic transport. $\sigma(q, \omega)$ does not display

the same banded feature as $\kappa(q, \omega)$ as prominently, presumably due to the fact that $[J_e(q = 0), H] \neq 0$, where the analogy with free fermions does not apply. Fig. 3 shows contour plots of $\sigma(q, \omega)$ and $\kappa(q, \omega)$ to better illustrate the banded nature of $\kappa(q, \omega)$ and enable comparison to $\sigma(q, \omega)$.

For the sake of comparison we also present numerical data for $\sigma(q, \omega)$ and $\kappa(q, \omega)$ of the NIM. The plots of these quantities are shown in Fig. 4. $[J_E(q = 0), H] \neq 0$ here and $\kappa(q = 0, \omega)$ is non-zero at $\omega \neq 0$. Both $\sigma(q = 0, \omega)$ and $\kappa(q = 0, \omega)$ display a finite non-analytic singularity at $\omega = 0$, which has been attributed to diffusion and non-linear hydrodynamics for the former [7]. In this system $\kappa(q, \omega)$ does not display the banded behavior of the IM and gradually goes to zero with increasing ω for all q . This is indicative of diffusion in this system, which we have verified by also computing the density-density correlators directly. The features (bumps) at large values of $q (= 5 - 8)$ and ω also appear in these correlators indicating the presence of interesting overdamped excitations, which will be investigated in detail elsewhere.

To conclude, we have demonstrated that the IM shows several signs of ballistic behavior as opposed to diffusion in the NIM. This has been illustrated through an extensive numerical calculation of finite temperature transport stiffnesses and dynamical conductivities. Further, the contribution of degenerate states coupled by the current has been shown to be insignificant to the Drude weight in the IM. The NIM seems to possess overdamped excitations at large momenta

The authors thank J. O. Haerter, D. A. Huse, J. E. Moore, M. R. Peterson and V. Oganesyan for discussions. S. M. thanks the DOE for support and the IBM SUR program. B.S.S. was supported by the DOE, BES under grant DE-FG02-06ER46319

-
- [1] B. S. Shastry, Phys. Rev. B **73**, 085117 (2006), URL http://physics.ucsc.edu/~sriram/papers_all/ksumrules_errors.
 - [2] T. Giamarchi and B. S. Shastry, Phys. Rev. B **51**, 10915 (1995).
 - [3] B. N. Narozhny, A. J. Millis, and N. Andrei, Phys. Rev. B **58**, R2921 (1998).
 - [4] X. Zotos, Phys. Rev. Lett. **82**, 1764 (1999), S. Fujimoto and N. Kawakami, Phys. Rev. Lett. **90**, 197202 (2003), J. V. Alvarez and C. Gros, Phys. Rev. Lett. **88**, 077203 (2002), J. Benz, T. Fukui, A. Klumper and C. Scheeren, J. Phys. Soc. Jpn. **74**, 181 (2005).
 - [5] F. Naef and X. Zotos, J. Phys. Cond. Mat **10**, L183 (1998).
 - [6] C. Stafford, A. J. Millis, and B. S. Shastry, Phys. Rev. B **43**, 13660 (1991).
 - [7] S. Mukerjee, V. Oganesyan, and D. A. Huse, Phys. Rev. B **73**, 035113 (2006).